CHEMISTRY & SUSTAINABILITY
CHEMSUSCHEM
ENERGY & MATERIALS

Accepted Article

Title: Shape Engineering of Biomass-Derived Nanoparticles from Hollow Spheres to Bowls via Solvent-Induced Buckling

Authors: Chunhong Chen, Xuefeng Li, Deng Jiang, Zhe Wang, and Yong Wang

To be cited as: *ChemSusChem* 10.1002/cssc.201801215

Link to VoR: http://dx.doi.org/10.1002/cssc.201801215

A Journal of
ChemPubSoc Europe

WILEY-VCH

www.chemsuschem.org

ChemSusChem 10.1002/cssc.201801215

Shape Engineering of Biomass-Derived Nanoparticles from Hollow Spheres to Bowls via Solvent-Induced Buckling

Chunhong Chen+, Xuefeng Li+, Jiang Deng, Zhe Wang, Yong Wang*

Dedication ((optional))

Abstract: To realize the asymmetry for the hollow carbonaceous nanostructures remains to be a great challenge, especially when biomass is chosen as the carbon resource via hydrothermal carbonization (HTC). Herein, a simple and straightforward solvent induced buckling strategy is demonstrated for the synthesis of asymmetric spherical and bowllike carbonaceous nanomaterials. The formation of the bowllike morphology was attributed to the buckling of the spherical shells induced by the dissolution of the oligomers. The bowllike particles made by this solvent-driven approach demonstrated a well-controlled morphology and a uniform particle size of ~360 nm. The obtained nanospheres and nanobowls can be loaded with CoS_2 nanoparticles to act as novel heterogeneous catalysts for the selective hydrogenation of aromatic nitro compounds. With the bowllike structure in hand, as expected, the CoS_2/nanobowls catalyst showed good tolerance to a wide scope of reducible groups and afforded both high activity and selectivity in almost all the tested substrates (14).

Introduction

Nanocontainers with controlled dimensions and intriguing morphologies have been regarded as an important family member of functional materials and attracted a great deal of attention in nanoscience and technology.[1-9] With the deepening of the nanoscience, controllable synthesis of asymmetric nanomaterials with special nonspherical geometric morphologies and compositions, such as nanobowls or nanoflasks, forms a new tendency, since these novel morphologies may endow new functionalities to the nanomaterials and create new opportunities in nanocatalysis or energy related fields.[10-17] Indeed, many interesting phenomena, such as improved catalytic performance, highly effective diffusivity, controllable and efficient encapsulation, and up-taking capacity for big guest molecules, have been observed already due to the unique single-hole hollow structural features compared to their closed-shell counterparts.[18-21]

Among the different types of asymmetric nanocontainers, the carbonaceous materials possess additional advantageous properties such as high chemical and thermal stability, good electrical conductivity, and accessible interior space etc.[22-26] Although tremendous efforts have been made in fabrication of hollow spheres, the strategy for the synthesis of asymmetric carbonaceous nanocontainers is still in imperfect start stage. Only a few methods have been reported for the rational synthesis of these materials and the most mature strategy of which is the templating method with such as resorcinol-formaldehyde (RE) resin as the carbon source and silica as hard template in general.[27-29] Although these methods are conceptually straightforward in producing nanocontainers, they suffer from fussy and tedious operating procedures, high cost, toxic reagents, and thus industrial unfeasible.[28, 30] Therefore, novel synthetic protocols, which are faster, cheaper, and greener, for the fabrication of asymmetric nanocontainers are especially welcome.

With growing global environmental awareness and increasing shortage of fossil resource, energy and sustainability issues nowadays have been seriously considered in designing synthetic strategies.[31] In this respect, materials chemists will be required to develop novel technologies and materials which are more efficient for the required applications and can minimize both short- and long-term impacts on the environment. Therefore, increased attention has been paid to the development of new and alternative carbons from renewable resources. Compared with organic polymer-derived (e.g., RE) carbon materials, biomass-derived carbonaceous materials synthesized from the hydrothermal carbonization (HTC) approach are of special interest in this consequence, as they are easy-processable, highly economical, and environmentally benign.[32-33] The HTC procedure is performed from renewable resources (e.g., glucose) at low temperatures (160-250 ºC) in aqueous medium under self-generated pressure. However, the HTC materials prepared in this straightforward water-based method are commonly irregular, micrometer-sized, spherical particles.[34-35] Our recent work demonstrated that the asymmetric, hollow, open, carbonaceous nanoflasks can be successfully fabricated by using a double templates HTC method from biomass, and the resulting asymmetric materials, flasklike carbon, exhibited a much higher energy storage ability for supercapacitors compared with the symmetric hollow counterpart. This study demonstrated the importance of preparing materials with desired morphology. To continue addressing critical challenges existed in synthesizing HTC carbon materials, new strategies to access materials with special morphology that could not be easily prepared previously, for example nanobowls, are necessary.

In this contribution, the difficult task of fabricating asymmetric bowllike nanoparticles from cheap biomass was accomplished

---

[a] C.Chen, X. Li, J. Deng, Z. Wang, Prof. Y. Wang
Advanced Materials and Catalysis Group, Institute of Catalysis, Zhejiang University
Hangzhou 310028, P. R. China.
E-mail: chemwy@zju.edu.cn

[+] These authors contributed equally to this work.

Supporting information for this article is given via a link at the end of the document.((Please delete this text if not appropriate))

10.1002/cssc.201801215

based on a “solvent induced buckling” method. The HTC process was firstly improved via a double-templating method to assist the formation of uniform asymmetric hollow sphere structure from inexpensive, harmless and naturally available sugars at 170 ºC followed by a post-solvent washing treatment to get the anisotropic bowllike nanoparticle. The unexpected versatile powers of this anisotropic bowllike materials were quickly recognized and contribute significant values to the products. For example, this HTC carbon was successfully coupled with metal salts (CoS_2) to produce novel nanohybrids, which served as a cheap and active catalyst for the selective hydrogenation of aromatic nitro compounds.[36-37]

Results and Discussion

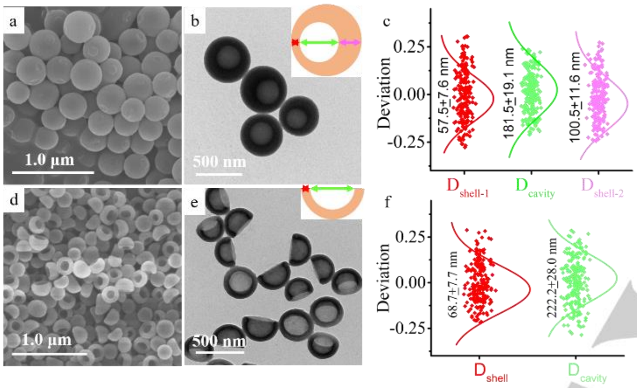

Figure 1. Morphologies characterization: SEM and TEM images for the non-centrosymmetric nanospheres (a, b) and nanobowls (d, e); Statistical distributions: the shell diameters and cavity diameters for nanospheres (c) and nanobowls (f).

The HTC reactions were performed at 170 ºC with glucose, a cheap and renewable sugar, chosen as carbon source and Poly (ethylene glycol)-block-poly (propylene glycol)-block-poly (ethylene glycol) (EO_{20}-PO_{70}-EO_{20}, P123) and sodium dodecyl sulfate (SDS) as double templates. Post solvents treatment after HTC is crucial for the formation of different morphologies as demonstrated in Figure 1. After 12 h HTC treatment, uniform hollow nanospheres with mean size around 340 nm are prepared by washing with water for several times (Figure 1a, b, c). The formation of these hollow nanospheres is mainly based on the cooperative formation of P123/SDS/glucose composite micelles under the acidic hydrothermal process.[38-39] It should be noted that the ratio of P123 will affect the final morphology of the products greatly, overloading of P123 would lead to the formation of flasklike carbon (Figure S1) as reported previous.[10] However, different from the hollow spheres reported previous, these hollow spheres are non-centrosymmetric with a thinner shell about 57 nm, a thicker shell about 100 nm, and a cavity diameter around 181 nm, as indicated in Figure 1b and c. The formation mechanism of these non-centrosymmetric structure will be discussed later. Interestingly, when further washed with ethanol after HTC and water washing, significant changes occurred, thereby giving products with uniform bowllike non-centrosymmetric hemispherical morphology as indicated by both TEM and SEM images (Figure 1d, e). These bowllike materials demonstrated a thickness of the shell and a diameter of hollow cavity of about 68 nm and 222 nm, respectively (Figure 1f).

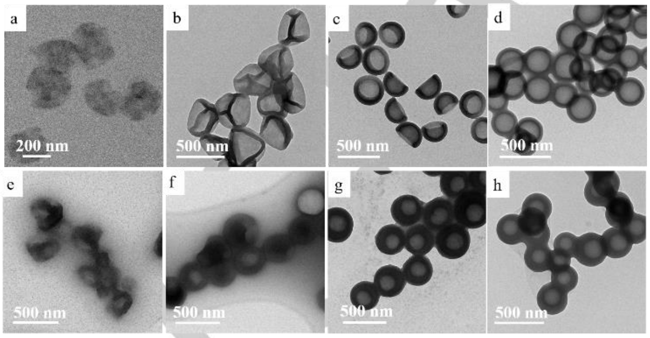

Figure 2. Shape evolution along with the hydrothermal reaction time: TEM images of samples fabricated with 6 h (a, e), 9 h (b, f), 12 h (c, g), and 24 h (d, h), respectively (a-d: samples were treated with deionized water and alcohol; e-h: the reaction solution freeze-dried directly).

To reveal the specific roles of the solvent treatment, the shape evolution was then studied by varying the hydrothermal reaction time, and the corresponding TEM images are listed in Figure 2 and SEM images listed in Figure S2. For comparison, as indicated in Figure 2, samples a, b, c, and d were treated with deionized water first and then with ethanol, and e, f, g, and h were samples freeze-dried directly after HTC. Images a, b, e, and f in Figure 2 are samples after 6, 9, 12, and 24 h HTC treatment, respectively. Owing to the sluggish reaction kinetics of the glucose HTC, only baby particles can be seen from these images, but even at this initial stage, differences can be observed when compared images b and image f in Figure 2. Obviously, Figure 2b demonstrated obviously buckling (crumpled) structure whereas Figure 2f showed hollow sphere morphology with one opening (Figure S2b). When the HTC time was prolonged to 12 hours, the above mentioned asymmetric hollow spheres and bowllike structure were observed, respectively. However, further prolonging to 24 hours, the samples after ethanol treatment turned to be relative uniform hollow spherical morphology, despite the freeze-dried counterparts still showed an asymmetric hollow spherical structure. These shape evolution against HTC time clearly revealed that the ethanol treatment of the HTC samples is a key factor that can control the final morphologies of the products. We then deduced this bowllike morphology obtained by buckling of the spherical shells. The buckling was induced by the dissolving of the oligomers (formation during the glucose HTC process) enclosed in the shells in the ethanol.[40-41] This may cause a stress comparable to an anisotropic pressure on a spherical airproof shell.[42] After post-buckling, the colloidal shells show bowllike morphology. Besides, this buckling resulted shapes is also affected by the HTC time. At the initial stage, for example 9 h, the hollow sphere texture is fragile, therefore the dissolving of the oligomers in the ethanol will lead to the collapse of the whole structure. While 12 h seems to be the suitable time to form the bowllike structure as both polymerization degree and shell thickness will increase with the increase of the HTC time.

Observed from the side of the bowllike structure, the interspace after buckling can be further observed (Figure S3 c). However, when further increasing the polymerization time, although some oligomers inside the shells were dissolved in the ethanol, the shells were still strong enough to resist the buckling press, therefore the intact hollow sphere like structure can be kept (Figure 2d). With this deduce of the oligomers inside the shells in hand, the asymmetric hollow spheres structure (freeze-dried directly after HTC, Figure 2g, h) can be reasonably attributed to the flowing of the oligomers inside the hollow shells. We then conducted the HTC reaction using a rotated homogeneous reactor instead of the still ones, the obtained samples still demonstrated asymmetric spherical morphology (Figure S4b). However, when these samples were further ultrasonically treated using water as solvent, obviously less asymmetric hollow shells were yielded (Figure S4c and Figure S5). These controlled experiments clearly indicated that the flowing oligomers inside the shells caused the asymmetric hollow spheres structure.

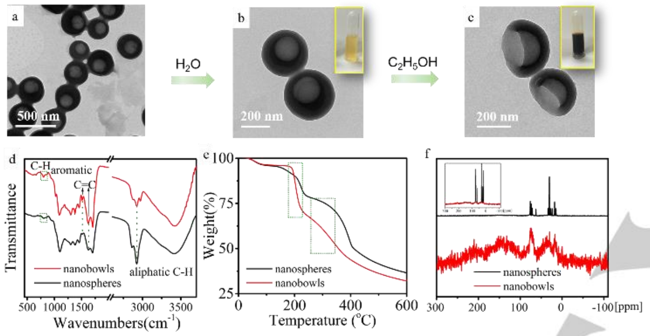

Figure 3. Morphological evolution: samples obtained by (a) freeze-dried reaction solution directly, (b) filtered with ultrapure water, and (c) further filtered with ethanol. Note: the inset pictures are the water filtrate (b) and ethanol filtrate (c). Characterization: the comparison of the FTIR spectra (d), the TGA (e), and ^{13}C direct polarization spectra (f) between the nanospheres and nanobowls.

Morphological evolution with the types of solvents were then examined in detail. After 12 h HTC treatment, the samples were divided into three parts, one was freeze-dried directly, another was filtered and washed with water, and the others were filtered and washed with both water and ethanol. The TEM images of these samples are listed in Figure 3. As expected, the samples without washing or washing with only water gave asymmetric spherical morphology, and the sample washed with additional ethanol demonstrated bowllike structure. It should be noted that the filtrates showed totally different color (Figure 3, inside image b and c), the water solution show pale yellow color and the ethanol solution gave brownish red color. These color differences may cause by the different dissolving ability of oligomers into the two different solvents. As an organic solvent, ethanol is a good solvent for oligomers, therefore more oligomers will be removed away by ethanol from the HTC products, and the residual samples should be the polymers with high polymerization degree. IR spectrum of the two structures were then conducted for comparison. The IR of the nanobowls showed increased aromatic C-H and C=C peaks but decreased aliphatic C-H peaks com-pared with the nanospheres counterparts, indicating different polymerization degree of the colloid shells. Furthermore, due to the coating of these oligomers, the decomposition rate of surfactants in nanospheres obviously slower than that in nanobowls (Figure 3e, Figure S6b). Solid state NMR results further convinced the residual of oligomers in the nano-sphere as showed in Figure 3f. The solvents as used were then extended to CH_3OH, CH_3CN, and $C_2H_4(OH)_2$, as showed in Figure S9, all these solvents lead to the formation of bowllike structure like ethanol. However, if the alcohols with longer side alky chain were used (such as C_4H_9OH, and $C_5H_{11}OH$), with the decreased oligomers solubility, both nanobowls and nanospheres were observed (Figure S10).

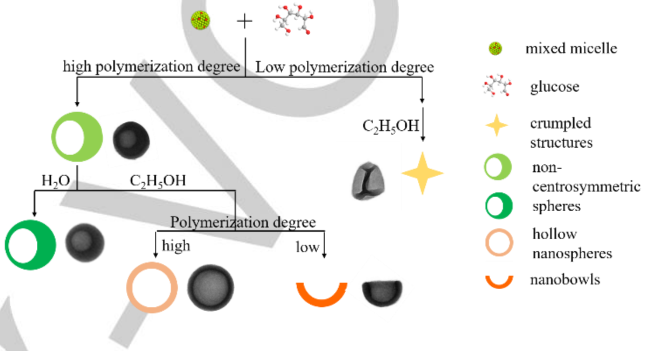

Figure 4. Schematic illustration of the different shape evolution paths via post-treatment of solvents.

On the basis of the above study, we proposed that the formation of the nanobowls and nanospheres in Figure 4. In the first stage, P123 and SDS acted as double templates and induced the formation of hollow spheres structures during the acidic HTC reaction. With different HTC time, the polymerization degree of the glucose will be different (Figure S11), and therefore leading to different morphology with or without ethanol treatment. For example, 9 h HTC of glucose and then washed with ethanol leads to the formation of crumpled structure for the dissolution of the large amount of oligomers at this early stage. When prolong the HTC time to 12 h, asymmetric hollow spheres are prepared with the help of the flowing oligomers inside the hollow spheres. Dissolving of the oligomers in ethanol induced the buckling of the shells and therefore the formation of asymmetric bowllike morphology. Simultaneously, the HTC time is also a key factor to affect the morphology of the final products, if the HTC time was prolonged to above 24 h (with enough high polymerization degree), even with the treatment of ethanol, only hollow spheres can be observed for the high carbonization degree of the shells.

To illustrate the usefulness of these novel materials with different morphologies, CoS_2 nanopartilces on nanospheres (CoS_2/NS) and nanobowls (CoS_2/NB) were then synthesized and selective hydrogenation of aromatic nitro compounds was tested. Powder X-ray diffraction (XRD) pattern of CoS_2/NS and CoS_2/NB validated the formation of high crysalline CoS_2 pyrite (JCPDS 41-1471). The morphologies of CoS_2/NB and CoS_2/NS composite materials have also been investigated by TEM (Figure 5). From the TEM images well-dispersed CoS_2 particles with mean size of 10.4 nm (CoS_2/NB) and 14.8 nm (CoS_2/NS) were found (Figure 5). It should be noted that the original morphology nanobowl and nanosphere remained well after coupling with CoS_2. The textural properties were further investigated using N_2 sorption isothermal analysis. CoS_2/NB and CoS_2/NS exhibited similar specific surface areas of 225 m^2 g^{-1} and 230 m^2 g^{-1}, respectively (Figure S12).

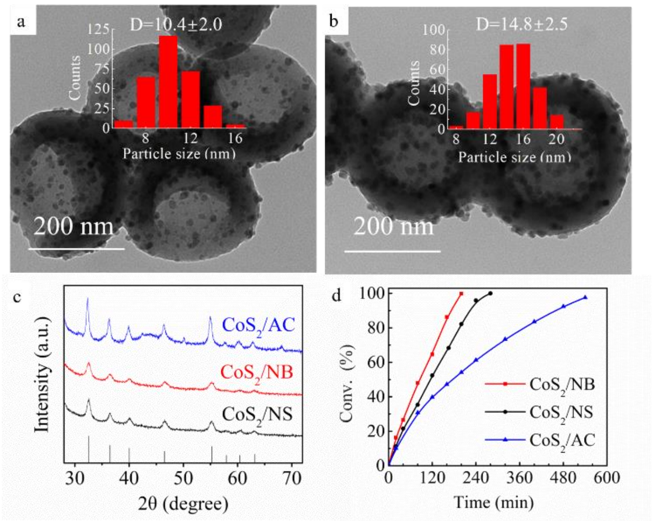

Figure 5. TEM (a, b) and (c) XRD patterns of CoS_2/NB, CoS_2/NS and CoS_2/AC. (d) Nitrobenzene reaction profile over CoS_2/NB, CoS_2/NS and CoS_2/AC. Reaction conditions: 2 mmol nitrobenzene, 30 mg catalyst, 30 mL methanol, 110 ºC, 3.0 MPa H_2.

Selective hydrogenation of aromatic nitro compounds is a general method for the synthesis of anilines, which are industrially important intermediates and fine chemicals. In the past years, the reduction of nitro compounds is readily carried out with various commercial catalysts, and noble metals such as Pt, Pd, or Ni are frequently used as heterogeneous catalysts for direct hydrogenation of nitro groups.[43-44] However, such processes have environmental and cost issues or selectivity problems. Undoubtedly, selective catalytic hydrogenation with hydrogen as the reductant represents one of the most critical technologies in chemical industry especially when Earth-abundant metals are used. The problems in the existing catalytic systems reinforce the need for new catalytic systems, including heterogeneous catalyst and clean reductant.[45-46]

Herein, CoS_2/NB and CoS_2/NS are active and afford remarkably high activity and selectivity towards the hydrogenation of nitrobenzene (Figure 5d). As shown, the reaction was almost completed in 200 min over CoS_2/NB and 280 min over CoS_2/NS. For comparison, we also prepared CoS_2/AC using commercial activated carbon as support. As shown in Figure 5, CoS_2/AC showed inferior activity for nitrobenzene hydrogenation compared with CoS_2/NB. From TEM images (Figure S13), obvious agglomerations of CoS_2 particles were observed on CoS_2/AC. According to TOF values (Table S2), it can be concluded that the high activity of CoS_2/NB is mainly due to its smaller particle size, which may be caused by unique bowllike structure.

The selective reduction of a nitro group with H_2 in the presence of other reducible functionalities is more challenging. We then examined the general scope of the catalytic hydrogenation of various substituted aromatic nitro compounds employing CoS_2/NB catalyst. As expected, CoS_2/NB showed good tolerance to a wide scope of reducible groups and afforded high conversion and excellent selectivity in almost all the tested substrates (Table 1).

Table 1. Selective hydrogenation of various substituted nitroarenes[a]

Entry	Substrate	Product	Conv.% [t(h)]	Sel. %
1	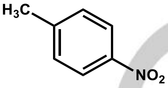	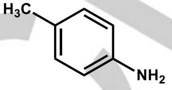	100[3]	>99
2	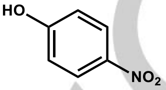	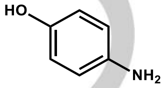	100[4.5]	>99
3	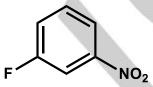	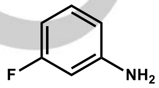	100[3]	>99
4	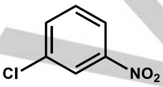	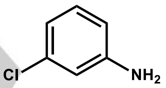	100[3]	>99
5	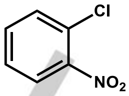	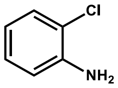	100[3]	>99
6	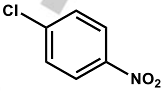	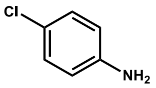	100[3]	99
7	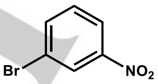	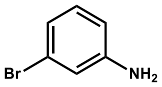	100[4]	>99
8	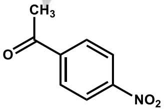	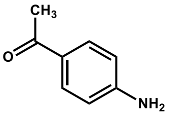	94[4]	>99
9[b]	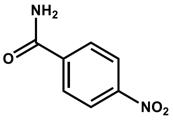	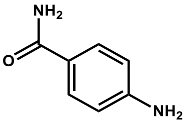	100[4.5]	>99
10[b]	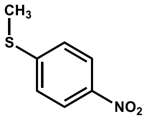	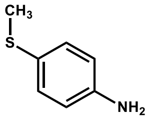	100[5]	>99
11[b]	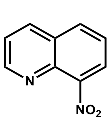	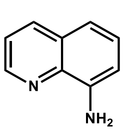	100[5]	>99
12[b]	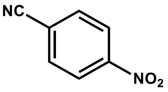	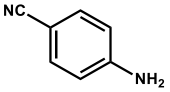	100[5]	99
13	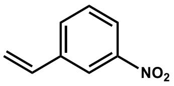	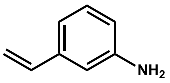	100[6]	99

[a] Reaction conditions: substrate (0.5 mmol), CoS_2/NB (1.4 mol% Co), methanol (3 mL), 110 ºC, 3 MPa H_2. [b] CoS_2/NB (2.8 mol% Co).

Conclusions

In conclusion, we have developed a novel method for creating asymmetric nanoparticles from cheap biomass via HTC. We propose a mechanism by which the cooperative formation of P123/SDS/glucose composite micelles leads to the fabricating of hollow nanospheres firstly, then the dissolution of oligomers formed during the glucose HTC process induced the buckling of the hollow shells and therefore the formation of the asymmetric nanomaterials. Meanwhile, these asymmetric nanomaterials can be used as efficient supports to deposit CoS_2 nanoparticles. The as made catalysts afford a remarkably high activity and selectivity towards the hydrogenation of aromatic nitro compounds. We envision this discovery of the biomass based asymmetric nanomaterials and their application in selective hydrogenation reactions may lead to further development of new architectures of catalyst support, thus allowing for more opportunities in material and heterogeneous catalysis field.

Experimental Section

Chemicals and Materials

SDS, glucose, and sulfur pow-der were bought from Aladdin reagent. P123 was purchased from Sigma-Aldrich. Anhydrous ethanol, Nitrobenzene, $Co(NO_3)_2{\cdot}6H_2O$, urea, and CS_2 were obtained from Sinopharm Chemical Reagent Co., Ltd. All gases (N_2, H_2) used for fabrication and reaction were with ultrahigh purity (99.999%).

Synthesis of the non-centrosymmetric nanospheres and nanobowls

An amount of 73mg SDS and 43 mg P123 were added into 20 ml of deionized water and stirred under ambient conditions for 2 h. After that, 40 mL of glucose solution (75 mg mL^{-1}) was introduced into the above solution with continuous stirring. Finally, the reaction solution was transferred into an autoclave and hydrothermally treated for 12 h at 170 °C. The hydrothermal products were collected by filtration, washed with plenty of deionized water (dried at 70 °C, denoted as non-centrosymmetric nanospheres). Further filtrated with anhydrous ethanol, and then dried at 70 °C, nanobowls were obtained.

Synthesis of CoS_2/nanobowls(nanospheres/activated carbon)

Typically, 0.2 g of nanobowls were added into 50 mL of deionized water and ultrasonically treated for 30 min to form a homogeneous suspension. 75 mg of $Co(NO_3)_2{\cdot}6H_2O$ and 150 mg of Urea were dissolved into the above suspension and stirred for 30 min. Then, the mixtures were transferred to an oil bath and reacted at 90 °C for 9 h under magnetic stirring. The resulting samples were washed with deionized water and ethanol for several times, followed by drying at 70 °C overnight. Finally, the composites were mixed with sulfur powder (mass ratio: 1:20) and calcinated at 450 °C for 2 h under N_2 atmospheres with the heating rate of 10 °C min^{-1}. The obtained samples were then rinsed with CS_2 to remove residual sulfur. After thoroughly washed with ethanol, CoS_2/nanobowls (CoS_2/NB) can be obtained.

Catalytic tests

Nitrobenzene hydrogenation experiments were performed in a 50 mL stainless steel autoclave equipped with a magnetic stirrer. In a typical process, the mixture of substrate, catalyst and solvent were added into the sealed autoclave. The reactor was purged with H_2 three times and then pressurized to 3.0 MPa with H_2. The reactor was placed in an oil-bath at 800 rpm and 110 °C for a certain time. After the reaction, the samples were determined by GC-FID and the products were identified by GC-MC.

Characterizations

Transmission electron microscopy (TEM) was carried out with a Hitachi HT-7700 electron microscope. Note: for TEM characterization, non-centrosymmetric nanospheres and nanobowls were dispersed in water and ethanol, respectively. Scanning electron microscopy (SEM) measurements were performed on a Hi-tachi SU-8010 electron microscope. The nitrogen adsorption - desorption analysis was performed at 77 K on a Micromeritics ASAP 2020 HD88, and the surface area was calculated using the BET equation. Powder x-ray diffraction (XRD) was measured on Model D/tex-Ultima TV using Cu Ka radiation (1.54 Å). Thermogravimetric analysis (TGA) of the samples was carried out using METTLER TOLEDO TGA at a heating rate of 10 °C min^{-1} under N_2 flow. Fourier transform infrared spectroscopy (FT-IR) spectra were recorded on a PerkinElmer FT-IR Spectrum GX in the spectral range of 400-4000cm^{-1} using the KBr disk method. Solid-State NMR measurements were performed using a Bruker Avance 400 III HD spectrometer (magnetic field strength 9.4 T) at resonance frequencies of 400.1 Hz for ^{1}H. The ^{13}C spectra were acquired with the ^{13}C excitation pulse at 90.9 kHz and the ^{1}H decoupling power at 98.0 kHz. Magic angle spinning experiments were conducted on a 3.2 mm HXY probe at a spin rate of 18 kHz. The ^{13}C signals were referenced to the methylene signal of adamantane at 38.5 ppm.

Acknowledgements ((optional))

Financial support from the National Natural Science Foundation of China (21622308, 91534114), the Key Program Supported by the Natural Science Foundation of Zhejiang Province, China (LZ18B060002), and the Fundamental Research Funds for the Central Universities (2017XZZX002-16) are greatly appreciated.

Keywords: asymmetry • nanospheres • nanobowls • soft-templating method • solvent-induced buckling

[1] C. N. Kaplan, W. L. Noorduin, L. Li, R. Sadza, L. Folkertsma, J. Aizenberg, L. Mahadevan, *Science* **2017**, *355*, 1395-1399.
[2] J.-B. Fan, Y. Song, H. Liu, Z. Lu, F. Zhang, H. Liu, J. Meng, L. Gu, S. Wang, L. Jiang, *Sci. Adv.* **2017**, *3*. e1603203.
[3] N. Doshi, A. S. Zahr, S. Bhaskar, J. Lahann, S. Mitragotri, *P Proc. Natl. Acad. Sci. USA* **2009**, *106*, 21495-21499.
[4] J. W. Kim, R. J. Larsen, D. A. Weitz, *Adv. Mater.* **2007**, *19*, 2005-2009.
[5] D. Liu, X. Peng, B. Wu, X. Zheng, T. T. Chuong, J. Li, S. Sun, G. D. Stucky, *J. Am. Chem. Soc.* **2015**, *137*, 9772-9775.
[6] J.-G. Park, J. D. Forster, E. R. Dufresne, *J. Am. Chem. Soc.* **2010**, *132*, 5960-5961.
[7] R. S. M. Rikken, H. Engelkamp, R. J. M. Nolte, J. C. Maan, J. C. M. van Hest, D. A. Wilson, P. C. M. Christianen, *Nat. Commun.* **2016**, *7*, 12606.
[8] P. A. Rupar, L. Chabanne, M. A. Winnik, I. Manners, *Science* **2012**, *337*, 559-562.
[9] A. van Blaaderen, *Nature* **2006**, *439*, 545-546.
[10] C. Chen, H. Wang, C. Han, J. Deng, J. Wang, M. Li, M. Tang, H. Jin, Y. Wang, *J. Am. Chem. Soc.* **2017**, *139*, 2657-2663.

[11] S.-H. Kim, A. D. Hollingsworth, S. Sacanna, S.-J. Chang, G. Lee, D. J. Pine, G.-R. Yi, *J. Am. Chem. Soc.* **2012**, *134*, 16115-16118.

[12] E. B. Mock, H. De Bruyn, B. S. Hawkett, R. G. Gilbert, C. F. Zukoski, *Langmuir* **2006**, *22*, 4037-4043.

[13] J. L. Perry, K. P. Herlihy, M. E. Napier, J. M. DeSimone, *Acc. Chem. Res.* **2011**, *44*, 990-998.

[14] S. She, Q. Li, B. Shan, W. Tong, C. Gao, *Adv. Mater.* **2013**, *25*, 5814-5818.

[15] R. Tamate, T. Ueki, R. Yoshida, *Angew. Chem. Int. Ed.* **2016**, *55*, 5179-5183; *Angew. Chem.* **2016**, *128*, 5265-5269.

[16] X. Wang, Y. Hou, L. Yao, M. Gao, M. Ge, *J. Am. Chem. Soc.* **2016**, *138*, 2090-2093.

[17] X. Zheng, M. Liu, M. He, D. J. Pine, M. Weck, *Angew. Chem. Int. Ed.* **2017**, *56*, 5507-5511; *Angew. Chem.* **2017**, *129*, 5599-5603.

[18] S. Hyuk Im, U. Jeong, Y. Xia, *Nat. Mater.* **2005**, *4*, 671-675.

[19] D. C. Hyun, P. Lu, S.-I. Choi, U. Jeong, Y. Xia, *Angew. Chem. Int. Ed.* **2013**, *52*, 10468-10471; *Angew. Chem.* **2013**, *125*, 10662-10665.

[20] X. Li, T. Zhao, Y. Lu, P. Wang, A. M. El-Toni, F. Zhang, D. Zhao, *Adv. Mater.* **2017**, *29*, 1701652.

[21] X. Li, L. Zhou, Y. Wei, A. M. El-Toni, F. Zhang, D. Zhao, *J. Am. Chem. Soc.* **2015**, *137*, 5903-5906.

[22] Y. Fang, Y. Lv, F. Gong, Z. Wu, X. Li, H. Zhu, L. Zhou, C. Yao, F. Zhang, G. Zheng, D. Zhao, *J. Am. Chem. Soc.* **2015**, *137*, 2808-2811.

[23] B. Y. Guan, L. Yu, X. W. Lou, *J. Am. Chem. Soc.* **2016**, *138*, 11306-11311.

[24] C. J. Hofer, R. N. Grass, M. Zeltner, C. A. Mora, F. Krumeich, W. J. Stark, *Angew. Chem. Int. Ed.* **2016***, 55,* 8761-8765*; Angew. Chem.* **2016***, 128,* 8905-8909.

[25] J. Liu, N. P. Wickramaratne, S. Z. Qiao, M. Jaroniec, *Nat. Mater.* **2015**, *14*, 763-774.

[26] R. Liu, S. M. Mahurin, C. Li, R. R. Unocic, J. C. Idrobo, H. Gao, S. J. Pennycook, S. Dai, *Angew. Chem. Int. Ed.* **2011***, 50,* 6799-6802*; Angew. Chem.* ***2011****, 123,* 6931-6934.

[27] F. Hu, H. Yang, C. Wang, Y. Zhang, H. Lu, Q. Wang, *Small* **2017**, *13*, 1602507.

[28] F. Pei, T. An, J. Zang, X. Zhao, X. Fang, M. Zheng, Q. Dong, N. Zheng, *Adv. Energy Mater.* **2016**, *6*, 1502539.

[29] H. Zhang, M. Yu, H. Song, O. Noonan, J. Zhang, Y. Yang, L. Zhou, C. Yu, *Chem. Mater.* **2015**, *27*, 6297-6304.

[30] Y. Chen, P. Xu, M. Wu, Q. Meng, H. Chen, Z. Shu, J. Wang, L. Zhang, Y. Li, J. Shi, *Adv. Mater.* **2014**, *26*, 4294-4301.

[31] M.-M. Titirici, R. J. White, N. Brun, V. L. Budarin, D. S. Su, F. del Monte, J. H. Clark, M. J. MacLachlan, *Chem. Soc. Rev.* **2015**, *44*, 250-290.

[32] B. Hu, K. Wang, L. Wu, S.-H. Yu, M. Antonietti, M.-M. Titirici, *Adv. Mater.* **2010**, *22*, 813-828.

[33] P. Zhang, J. Yuan, T.-P. Fellinger, M. Antonietti, H. Li, Y. Wang, *Angew. Chem. Int. Ed.* **2013***, 52,* 6028-6032*; Angew. Chem.* **2013***, 125,* 6144-6148.

[34] M. Sevilla, A. B. Fuertes, *Chem. Eur. J.* **2009**, *15*, 4195-4203.

[35] M.-M. Titirici, M. Antonietti, N. Baccile, *Green Chem.* **2008**, *10*, 1204-1212.

[36] R. M. Bullock, *Science* **2013**, *342*, 1054-1055.

[37] R. V. Jagadeesh, A.-E. Surkus, H. Junge, M.-M. Pohl, J. Radnik, J. Rabeah, H. Huan, V. Schünemann, A. Brückner, M. Beller, *Science* **2013**, *342*, 1073-1076.

[38] R. Ganguly, V. K. Aswal, P. A. Hassan, I. K. Gopalakrishnan, S. K. Kulshreshtha, *J. Phys. Chem. B* **2006**, *110*, 9843-9849.

[39] X. Xin, G. Xu, Y. Wang, H. Mao, Z. Zhang, *Eur. Polym. J.* **2008**, *44*, 3246-3255.

[40] D.-S. Bin, Z.-X. Chi, Y. Li, K. Zhang, X. Yang, Y.-G. Sun, J.-Y. Piao, A.-M. Cao, L.-J. Wan, *J. Am. Chem. Soc.* **2017**, *139*, 13492-13498.

[41] Q. Yue, J. Li, Y. Zhang, X. Cheng, X. Chen, P. Pan, J. Su, A. A. Elzatahry, A. Alghamdi, Y. Deng, D. Zhao, *J. Am. Chem. Soc.* **2017**, *139*, 15486-15493.

[42] C. Quilliet, C. Zoldesi, C. Riera, A. van Blaaderen, A. Imhof, *Eur. Phys. J. E* **2008**, *27*, 13-20.

[43] H. Wei, X. Liu, A. Wang, L. Zhang, B. Qiao, X. Yang, Y. Huang, S. Miao, J. Liu, T. Zhang, *Nat. Commun.* **2014**, *5*, 5634.

[44] F. A. Westerhaus, R. V. Jagadeesh, G. Wienhöfer, M.-M. Pohl, J. Radnik, A.-E. Surkus, J. Rabeah, K. Junge, H. Junge, M. Nielsen, A. Brückner, M. Beller, *Nat. Chem.* **2013**, *5*, 537-543.

[45] L. Liu, P. Concepción, A. Corma, *J. Catal.* **2016**, *340*, 1-9.

[46] Z. Wei, S. Mao, F. Sun, J. Wang, B. Mei, Y. Chen, H. Li, Y. Wang, *Green Chem.* **2018**, *19*, 18-43**.**

Entry for the Table of Contents (Please choose one layout)

Layout 1:

FULL PAPER

By coupling with soft template method using biomass as precursor, we can synthesize non-centrosymmetric nanospheres. Furthermore, post-treatment with different solvents, it can remain the same nanospheres or realize a shapeshift into nanobowls

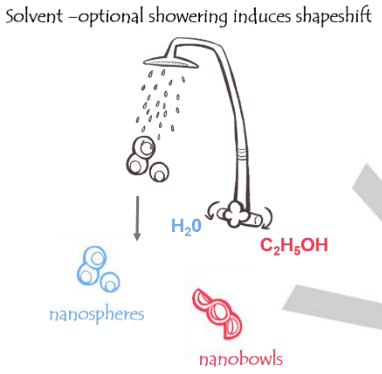

*Chunhong Chen+, Xuefeng Li+, Jiang Deng, Zhe Wang, Yong Wang**

Page No. – Page No.

Shape Engineering of Biomass-Derived Nanoparticles from Hollow Spheres to Bowls via Solvent-Induced Buckling